Catal Lett (2008) 124:262–267
DOI 10.1007/s10562-008-9450-4

Effect of Oxygen Capacity and Oxygen Mobility of Pure Bismuth Molybdate and Multicomponent Bismuth Molybdate on their Catalytic Performance in the Oxidative Dehydrogenation of *n*-Butene to 1,3-Butadiene

Ji Chul Jung · Howon Lee · Heesoo Kim · Young-Min Chung · Tae Jin Kim · Seong Jun Lee · Seung-Hoon Oh · Yong Seung Kim · In Kyu Song

Received: 3 February 2008 / Accepted: 19 February 2008 / Published online: 6 March 2008

Abstract Pure bismuth molybdate (γ-Bi_2MoO_6) and multicomponent bismuth molybdate ($Co_9Fe_3Bi_1Mo_{12}O_{51}$) catalysts were prepared by a co-precipitation method, and were applied to the oxidative dehydrogenation of *n*-butene to 1,3-butadiene. The $Co_9Fe_3Bi_1Mo_{12}O_{51}$ catalyst showed a better catalytic performance than the γ-Bi_2MoO_6 catalyst in terms of conversion of *n*-butene and yield for 1,3-butadiene, indicating that the multicomponent bismuth molybdate was more efficient than the pure bismuth molybdate in the oxidative dehydrogenation of *n*-butene. It was revealed that the crucial factor determining the catalytic performance of Bi–Mo-based catalyst in the oxidative dehydrogenation of *n*-butene is not the amount of oxygen in the catalyst involved in the reaction (oxygen capacity) but the intrinsic mobility of oxygen in the catalyst involved in the reaction (oxygen mobility). The enhanced catalytic performance of $Co_9Fe_3Bi_1Mo_{12}O_{51}$ was due to its facile oxygen mobility.

Keywords Pure bismuth molybdate · Multicomponent bismuth molybdate · Oxygen mobility · Oxidative dehydrogenation · *n*-Butene

J. C. Jung · H. Lee · H. Kim · I. K. Song (✉)
School of Chemical and Biological Engineering, Institute of Chemical Processes, Seoul National University, Shinlim-dong, Kwanak-ku, Seoul 151-744, South Korea
e-mail: inksong@snu.ac.kr

Y.-M. Chung · T. J. Kim · S. J. Lee · S.-H. Oh · Y. S. Kim
SK Energy Corporation, Yuseong-ku, Daejeon 305-712, South Korea

1 Introduction

Selective oxidation of olefins, such as oxidation of propylene to acrolein, ammoxidation of propylene to acrylonitrile, and oxidative dehydrogenation of *n*-butene to 1,3-butadiene, is one of the challenging research areas in petrochemical industries due to its practical importance for large-scale synthesis of various chemical intermediates [1–3]. In particular, the oxidative dehydrogenation of *n*-butene has attracted much attention as a promising process for producing 1,3-butadiene [4–7], an important raw material for manufacturing a large number of chemicals such as ABS (acrylonitrile–butadiene–styrene), BR (butadiene rubber), and SBR (styrene–butadiene rubber) [8, 9]. The oxidative dehydrogenation of *n*-butene has many advantages over the conventional naphtha cracking process in producing 1,3-butadiene, because this process can be operated as a single unit and is independent of the naphtha cracking unit. Furthermore, no additional major naphtha cracking products such as ethylene and propylene are produced in the oxidative dehydrogenation of *n*-butene [4–6, 10–14].

Bi–Mo-based catalysts such as pure bismuth molybdates and multicomponent bismuth molybdates have been widely investigated as efficient catalysts for the oxidative dehydrogenation of *n*-butene to 1,3-butadiene [15–17]. Although three types of pure bismuth molybdate catalysts (α-$Bi_2Mo_3O_{12}$, β-$Bi_2Mo_2O_9$, and γ-Bi_2MoO_6) have been considered for the oxidative dehydrogenation of *n*-butene [18–20], multicomponent bismuth molybdate catalysts with various metal components have been mainly employed for this reaction to improve the low catalytic activity of pure bismuth molybdates [21, 22]. However, it is not still clear why the multicomponent bismuth molybdate catalysts are more active than the pure bismuth

molybdate catalysts in the oxidative dehydrogenation of *n*-butene. Furthermore, only a few studies on the multicomponent bismuth molybdate catalysts were reported in the literature [17, 23–25], due to the difficulty in understanding their complicated compositions and structures. Therefore, an attempt to elucidate the different catalytic performance of pure bismuth molybdate and multicomponent bismuth molybdate catalysts in the oxidative dehydrogenation of *n*-butene would be worthwhile.

It was observed in our previous work [26] that γ-Bi_2MoO_6 showed the best catalytic performance in the oxidative dehydrogenation of *n*-butene, among three types of pure bismuth molybdates (α-$Bi_2Mo_3O_{12}$, β-$Bi_2Mo_2O_9$, and γ-Bi_2MoO_6). It is known that the fundamental structure of multicomponent bismuth molybdate catalysts is composed of four elements including divalent metal (M^{II}), trivalent metal (M^{III}), bismuth, and molybdenum [17, 24]. Although a number of multicomponent bismuth molybdate catalysts can be formed depending on the constituent metal components and their compositions, it was revealed that $Co_9Fe_3Bi_1Mo_{12}O_{51}$ served as an efficient multicomponent bismuth molybdate catalyst for the oxidative dehydrogenation of *n*-butene [27]. In this work, therefore, γ-Bi_2MoO_6 and $Co_9Fe_3Bi_1Mo_{12}O_{51}$ were chosen as model catalysts to elucidate the different catalytic performance of pure bismuth molybdate and multicomponent bismuth molybdate in the oxidative dehydrogenation of *n*-butene.

It is well known that the oxidative dehydrogenation of *n*-butene follows the Mars-van Krevelen mechanism [28–31]. According to this mechanism, oxygen in the catalyst directly reacts with *n*-butene, and in turn, oxygen in the gas phase makes up oxygen vacancy in the catalyst. This indicates that metal component in the catalyst does not directly take part in the reaction, although the nature of oxygen involved in the reaction can vary depending on the identity of metal component bonded to the oxygen. Considering the fact that oxygen in the catalyst directly reacts with *n*-butene in the oxidative dehydrogenation of *n*-butene, it can be inferred that the amount of oxygen in the catalyst involved in the reaction (oxygen capacity) and/or the intrinsic mobility of oxygen in the catalyst involved in the reaction (oxygen mobility) may serve as one of the crucial factors determining the catalytic performance in this reaction. Therefore, this work was focused on the nature of oxygen in the catalyst, with an aim of elucidating the catalytic performance of Bi–Mo-based catalysts in the oxidative dehydrogenation of *n*-butene.

In this work, γ-Bi_2MoO_6 and $Co_9Fe_3Bi_1Mo_{12}O_{51}$ catalysts were prepared by a co-precipitation method, and were applied to the oxidative dehydrogenation of *n*-butene to 1,3-butadiene. The oxidative dehydrogenation of *n*-butene over γ-Bi_2MoO_6 and $Co_9Fe_3Bi_1Mo_{12}O_{51}$ catalysts was also carried out in the absence of oxygen feed, with an aim of measuring the oxygen capacity of the catalyst (the amount of oxygen in the catalyst consumed for the reaction). XPS measurements were conducted to determine the oxygen mobility of the catalyst (the intrinsic mobility of oxygen in the catalyst involved in the reaction). The effect of oxygen capacity and oxygen mobility of γ-Bi_2MoO_6 and $Co_9Fe_3Bi_1Mo_{12}O_{51}$ on their catalytic performance in the oxidative dehydrogenation of *n*-butene was investigated.

2 Experimental

2.1 Preparation of γ-Bi_2MoO_6 and $Co_9Fe_3Bi_1Mo_{12}O_{51}$ Catalysts

γ-Bi_2MoO_6 catalyst was prepared by a co-precipitation method. 15.9 g of bismuth nitrate ($Bi(NO_3)_3{\cdot}5H_2O$, Sigma–Aldrich) was dissolved in 20 mL of distilled water that had been acidified with 6 mL of concentrated nitric acid. The solution was then added dropwise into 60 mL of an aqueous solution containing 2.9 g of ammonium molybdate ($(NH_4)_6Mo_7O_{24}{\cdot}4H_2O$, Sigma–Aldrich) under vigorous stirring. During the co-precipitation step, pH of the mixed solution was maintained at 3 using an aqueous ammonia solution (3N). After stirring the resulting solution vigorously at room temperature for 1 h, the precipitate was filtered to obtain a solid product. The solid product was dried overnight at 110 °C, and then it was calcined at 475 °C for 5 h in an air stream to yield the γ-Bi_2MoO_6 catalyst.

$Co_9Fe_3Bi_1Mo_{12}O_{51}$ catalyst was also prepared by a co-precipitation method. 1.5 g of bismuth nitrate ($Bi(NO_3)_3{\cdot}5H_2O$, Sigma–Aldrich) was dissolved in 10 mL of distilled water that had been acidified with 3 mL of concentrated nitric acid. The solution was then added into 100 mL of an aqueous solution containing 7.9 g of cobalt nitrate ($Co(NO_3)_2{\cdot}6H_2O$, Sigma–Aldrich) and 3.7 g of ferric nitrate ($Fe(NO_3)_3{\cdot}9H_2O$, Sigma–Aldrich) to obtain a mixed nitrate solution. The mixed nitrate solution was added dropwise into 50 mL of an aqueous solution containing 6.4 g of ammonium molybdate ($(NH_4)_6Mo_7O_{24}{\cdot}4H_2O$, Sigma–Aldrich) under vigorous stirring. After stirring the mixed solution at room temperature for 1 h, a solid product was obtained by evaporation. The solid product was dried overnight at 175 °C, and then it was calcined at 475 °C for 5 h in an air stream to yield the $Co_9Fe_3Bi_1Mo_{12}O_{51}$ catalyst.

2.2 Characterization

Formation of γ-Bi_2MoO_6 and $Co_9Fe_3Bi_1Mo_{12}O_{51}$ catalysts was confirmed by XRD (MAC Science, M18XHF-SRA) measurements. Atomic ratios of constituent metal components

in the prepared catalysts were determined by ICP-AES (Shimadz, ICP-1000IV) analyses. Surface areas of the catalysts were measured using a BET apparatus (Micromeritics, ASAP 2010). XPS analyses (Thermo VG, Sigma Probe) for measuring the binding energies of O 1s of γ-Bi_2MoO_6 and $Co_9Fe_3Bi_1Mo_{12}O_{51}$ catalysts were conducted to determine the oxygen mobility of the catalysts. Binding energies of O 1s were calibrated using C 1s peak (284.5 eV) as a reference.

2.3 Oxidative Dehydrogenation of *n*-Butene

Oxidative dehydrogenation of *n*-butene to 1,3-butadiene was carried out in a continuous flow fixed-bed reactor in the presence of air and steam. Each catalyst (0.5 g) was pretreated at 470 °C for 1 h with an air stream (16 mL/min). Water was sufficiently vaporized by passing through a pre-heating zone and was continuously fed into the reactor together with *n*-butene and air. Feed composition was fixed at *n*-butene:O_2:steam=1:0.75:15. C_4 raffinate-3 containing 72.5 wt% *n*-butene (1-butene (14.2 wt%) + *trans*-2-butene (38.3 wt%) + *cis*-2-butene (20.0 wt%)) was used as a *n*-butene source, and air was used as an oxygen source (nitrogen in air served as a carrier gas). C_4 raffinate-3 was composed of 72.5 wt% *n*-butene, 26.9 wt% *n*-butane, 0.4 wt% cyclobutane, 0.1 wt% methyl cyclopropane, and 0.1 wt% residue. The catalytic reaction was carried out at 420 °C. GHSV (gas hourly space velocity) was fixed at 500 h^{-1} on the basis of *n*-butene. Reaction products were periodically sampled and analyzed with gas chromatographs. Conversion of *n*-butene and selectivity for 1,3-butadiene were calculated on the basis of carbon balance as follows. Yield for 1,3-butadiene was calculated by multiplying conversion and selectivity.

$$\text{Conversion of } n\text{-butane} = \frac{\text{moles of } n-\text{butene reacted}}{\text{moles of } n\text{-butene supplied}} \quad (1)$$

$$\text{Selectivity for 1,3-butadiene} = \frac{\text{moles of } 1,3-\text{butadiene formed}}{\text{moles of } n\text{-butene reacted}} \quad (2)$$

3 Results and Discussion

3.1 Formation of γ-Bi_2MoO_6 and $Co_9Fe_3Bi_1Mo_{12}O_{51}$ Catalysts

Successful formation of γ-Bi_2MoO_6 and $Co_9Fe_3Bi_1Mo_{12}O_{51}$ catalysts was confirmed by XRD and ICP-AES measurements. Figure 1 shows the XRD patterns of γ-Bi_2MoO_6 and $Co_9Fe_3Bi_1Mo_{12}O_{51}$ catalysts. Each phase was identified by its characteristic diffraction peaks using JCPDS. As shown in Fig. 1, γ-Bi_2MoO_6 catalyst retained a pure γ-Bi_2MoO_6 phase, while $Co_9Fe_3Bi_1Mo_{12}O_{51}$ catalyst was composed of four major mixed phases of β-$CoMoO_4$, α-$CoMoO_4$, $Fe_2(MoO_4)_3$, and γ-Bi_2MoO_6. These XRD patterns were in good agreement with those reported in previous works [3, 4, 17], indicating the successful formation of γ-Bi_2MoO_6 and $Co_9Fe_3Bi_1Mo_{12}O_{51}$ catalysts. Bi:Mo atomic ratio in the γ-Bi_2MoO_6 catalyst and Co:Fe:Bi:Mo atomic ratio in the $Co_9Fe_3Bi_1Mo_{12}O_{51}$ catalyst determined by ICP-AES analyses were found to be 2.0:1.0 and 9.0:3.2:1.0:11.4, respectively. These values were well consistent with the theoretical values. This result also supports that γ-Bi_2MoO_6 and $Co_9Fe_3Bi_1Mo_{12}O_{51}$ catalysts were successfully prepared in this work. BET surface areas of γ-Bi_2MoO_6 and $Co_9Fe_3Bi_1Mo_{12}O_{51}$ catalysts were very low with no significant difference (3.5 and 2.3 m^2/g, respectively), as reported in previous works [22, 32].

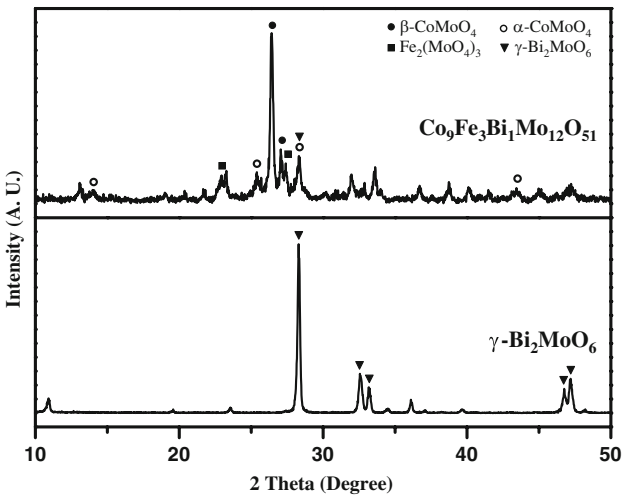

Fig. 1 XRD patterns of γ-Bi_2MoO_6 and $Co_9Fe_3Bi_1Mo_{12}O_{51}$ catalysts

3.2 Catalytic Performance in the Oxidative Dehydrogenation of *n*-Butene

Figure 2 shows the catalytic performance of γ-Bi_2MoO_6 and $Co_9Fe_3Bi_1Mo_{12}O_{51}$ in the oxidative dehydrogenation of *n*-butene at 420 °C after a 6 h-reaction. In the catalytic reaction, CO_2 was mainly produced as a by-product. Conversion of *n*-butene obtained with $Co_9Fe_3Bi_1Mo_{12}O_{51}$ catalyst was much higher than that obtained with γ-Bi_2MoO_6 catalyst, while selectivity for 1,3-butadiene over $Co_9Fe_3Bi_1Mo_{12}O_{51}$ catalyst was slightly lower than that over γ-Bi_2MoO_6 catalyst. As a consequence, the $Co_9Fe_3Bi_1Mo_{12}O_{51}$ catalyst exhibited a higher yield for 1,3-butadiene than the γ-Bi_2MoO_6 catalyst. This result indicates that the multicomponent bismuth molybdate is more efficient than the pure bismuth molybdate in the oxidative dehydrogenation of *n*-butene.

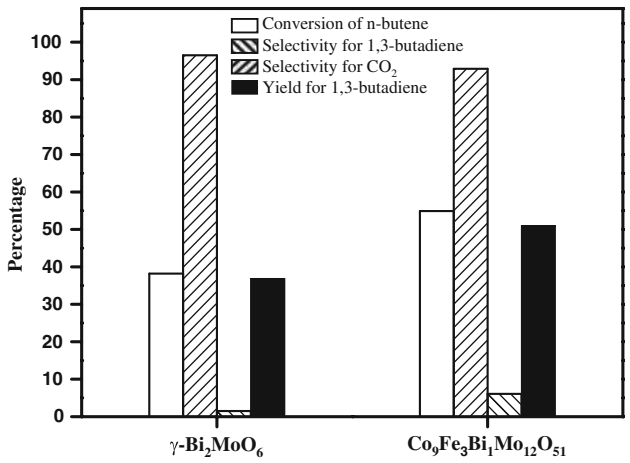

Fig. 2 Catalytic performance of γ-Bi_2MoO_6 and $Co_9Fe_3Bi_1Mo_{12}O_{51}$ in the oxidative dehydrogenation of *n*-butene to 1,3-butadiene at 420 °C after a 6 h-reaction

3.3 Oxygen Capacity of γ-Bi_2MoO_6 and $Co_9Fe_3Bi_1Mo_{12}O_{51}$ Catalysts

Oxidative dehydrogenation of *n*-butene was carried out in the absence of the oxygen feed in order to determine the oxygen capacity of the catalyst (the amount of oxygen in the catalyst consumed for the reaction). Figure 3 shows the yield for 1,3-butadiene over γ-Bi_2MoO_6 and $Co_9Fe_3Bi_1Mo_{12}O_{51}$ catalysts with time on stream obtained in the absence of oxygen feed in the oxidative dehydrogenation of *n*-butene at 420 °C. Both γ-Bi_2MoO_6 and $Co_9Fe_3Bi_1Mo_{12}O_{51}$ catalysts in the absence of oxygen feed exhibited comparable catalytic activities to those in the presence of oxygen feed at the initial stage. However, yield for 1,3-butadiene in the absence of oxygen feed gradually decreased with increasing reaction time, and finally, reached zero after a 3 h-reaction. This indicates that both catalysts consumed lattice oxygen for the reaction in the absence of oxygen feed, in good agreement with the Mars-van Krevelen mechanism, which has been generally accepted for the oxidative dehydrogenation of *n*-butene [28–31]. It also means that the whole lattice oxygen that could be utilized for the reaction were completely consumed in both catalysts after a 3 h-reaction in the absence of oxygen feed. Therefore, it can be inferred that the area obtained by integrating the curve of 1,3-butadiene yield reflects the total amount of lattice oxygen in the catalyst consumed for the reaction (the oxygen capacity of the catalyst).

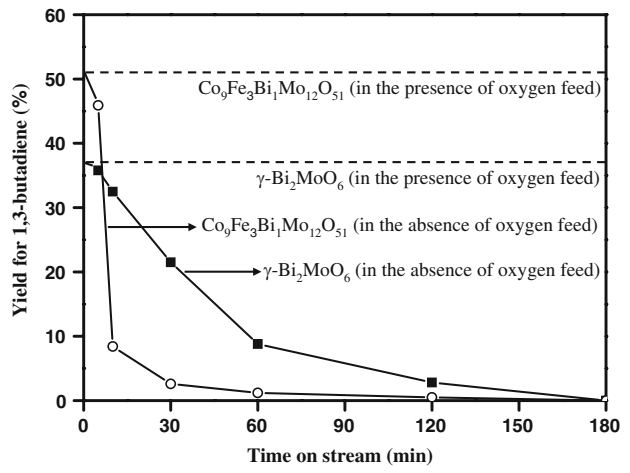

Fig. 3 Yield for 1,3-butadiene over γ-Bi_2MoO_6 and $Co_9Fe_3Bi_1Mo_{12}O_{51}$ catalysts with time on stream obtained in the absence of oxygen feed in the oxidative dehydrogenation of *n*-butene at 420 °C

It is interesting to note that yield for 1,3-butadiene over $Co_9Fe_3Bi_1Mo_{12}O_{51}$ catalyst decreased more rapidly than that over γ-Bi_2MoO_6 catalyst with respect to reaction time in the absence of oxygen feed, leading to a lower integration area of 1,3-butadiene yield over $Co_9Fe_3Bi_1Mo_{12}O_{51}$ catalyst. This indicates that the $Co_9Fe_3Bi_1Mo_{12}O_{51}$ catalyst retained a smaller oxygen capacity than the γ-Bi_2MoO_6 catalyst.

3.4 Oxygen Mobility of γ-Bi_2MoO_6 and $Co_9Fe_3Bi_1Mo_{12}O_{51}$ Catalysts

It is known that XPS is one of the powerful tools for measuring the oxygen mobility of the catalyst [33, 34]. We

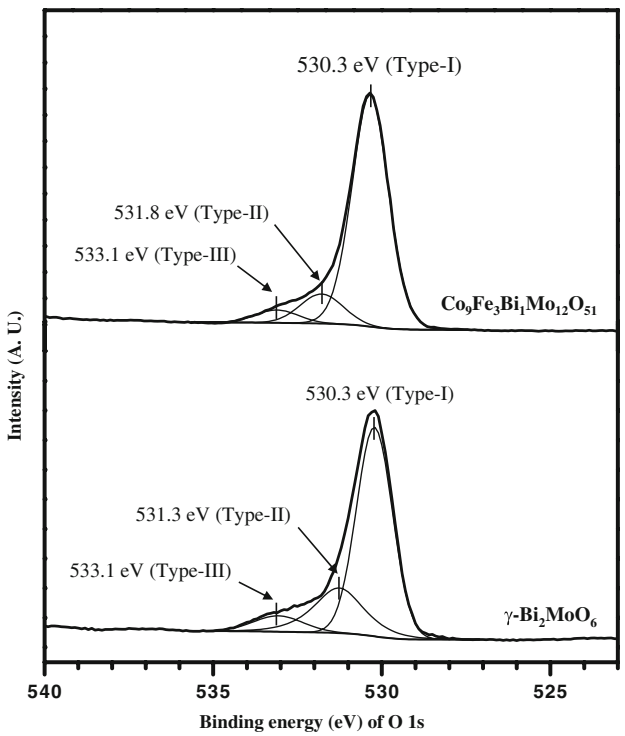

Fig. 4 XPS spectra for O 1s of γ-Bi_2MoO_6 and $Co_9Fe_3Bi_1Mo_{12}O_{51}$ catalysts

measured the binding energies of O 1s of γ-Bi_2MoO_6 and $Co_9Fe_3Bi_1Mo_{12}O_{51}$ catalysts in order to determine the oxygen mobility of the catalysts. Figure 4 shows the XPS spectra for O 1s of γ-Bi_2MoO_6 and $Co_9Fe_3Bi_1Mo_{12}O_{51}$ catalysts. Deconvolution of XPS spectra reveals that there are three types of oxygen species in both catalysts (denoted as type-I, II, and III in the order of increasing binding energy). What is interesting is that the binding energies of type-I and III oxygen species are the same each other in both catalysts, while those of type-II oxygen species are different in both catalysts. Type-I oxygen with the lowest binding energy (530.3 eV) corresponds to the oxygen species strongly bonded to the metal component in the catalyst. On the other hand, type-III oxygen with the highest binding energy (533.1 eV) is believed to be the oxygen species weakly bonded on the catalyst surface. The above results indicate that type-I and III oxygens are not the major oxygen species responsible for the oxidative dehydrogenation of *n*-butene. In our previous work investigating the oxygen mobility of $Ni_9Fe_3Bi_1Mo_{12}O_{51}$ catalysts prepared at different pH [35], it was revealed that only the binding energy of type-II oxygen reflected the oxygen mobility of the multicomponent bismuth molybdate catalyst. In this work, therefore, the binding energy of type-II oxygen was used as an index for the oxygen mobility of the catalyst.

The binding energy of O 1s of the metal oxide catalysts increases with decreasing valence electron density of lattice oxygen. This indicates that metal-oxygen bonds in the catalyst would be weakened with increasing binding energy of O 1s, making the lattice oxygen more active and mobile [34]. In other words, the higher binding energy of O 1s corresponds to the higher oxygen mobility. As shown in Fig. 4, the binding energy of type-II oxygen of $Co_9Fe_3Bi_1Mo_{12}O_{51}$ catalyst (531.8 eV) was much higher than that of γ-Bi_2MoO_6 catalyst (531.3 eV), indicating that the $Co_9Fe_3Bi_1Mo_{12}O_{51}$ catalyst retained a higher oxygen mobility than the γ-Bi_2MoO_6 catalyst.

It is known that bismuth molybdates are located on the surface of the catalyst and serve as active phases in the multicomponent bismuth molybdate catalyst system, while divalent and trivalent metal molybdates are concentrated in the bulk of the catalyst [17]. It has also been reported that the divalent and trivalent metal molybdates in the bulk of the catalyst not only act as supports for the active components but also facilitate the migration of active oxygen species to the bismuth molybdates on the catalyst surface, leading to an enhanced oxygen mobility of multicomponent bismuth molybdate catalysts [22]. Therefore, it is believed that the enhanced oxygen mobility of $Co_9Fe_3Bi_1Mo_{12}O_{51}$ catalyst was due to the facile migration of active oxygen species to the catalyst surface.

The $Co_9Fe_3Bi_1Mo_{12}O_{51}$ catalyst with high oxygen mobility and small oxygen capacity showed a better catalytic performance than the γ-Bi_2MoO_6 catalyst in the oxidative dehydrogenation of *n*-butene (Figs. 2–4). This indicates that the oxygen mobility rather than the oxygen capacity played a key role in determining the catalytic performance in the oxidative dehydrogenation of *n*-butene. Therefore, it is concluded that the crucial factor determining the catalytic performance in the oxidative dehydrogenation of *n*-butene is not the amount of oxygen in the catalyst consumed for the reaction (oxygen capacity) but the intrinsic mobility of oxygen in the catalyst involved in the reaction (oxygen mobility). Thus, the enhanced catalytic performance of $Co_9Fe_3Bi_1Mo_{12}O_{51}$ was attributed to its facile oxygen mobility.

4 Conclusions

γ-Bi_2MoO_6 and $Co_9Fe_3Bi_1Mo_{12}O_{51}$ catalysts were prepared by a co-precipitation method, and were applied to the oxidative dehydrogenation of *n*-butene to 1,3-butadiene. Successful formation of the catalysts was well confirmed by XRD and ICP-AES analyses. Conversion of *n*-butene and yield for 1,3-butadiene over $Co_9Fe_3Bi_1Mo_{12}O_{51}$ catalyst were much higher than those over γ-Bi_2MoO_6 catalyst, indicating that the multicomponent bismuth molybdate was more efficient than the pure bismuth molybdate in the oxidative dehydrogenation of *n*-butene. When considering the fact that the $Co_9Fe_3Bi_1Mo_{12}O_{51}$ catalyst retained a higher oxygen mobility and a smaller oxygen capacity than the γ-Bi_2MoO_6 catalyst, it is concluded that the oxygen mobility played a key role in determining the catalytic performance of Bi–Mo-based catalyst in the oxidative dehydrogenation of *n*-butene. The enhanced catalytic performance of $Co_9Fe_3Bi_1Mo_{12}O_{51}$ was due to its facile oxygen mobility.

Acknowledgment The authors wish to acknowledge support from the Korea Energy Management Corporation (2005-01-0090-3-010).

References

1. Burrington JD, Kartisek CT, Grasselli RK (1980) J Catal 63:235
2. Kim YH, Yang HS (2000) Korean J Chem Eng 17:357
3. Soares APV, Dimitrov LD, Oliveira MCA, Hilaire L, Portela MF, Grasselli RK (2003) Appl Catal A 253:191
4. Batist PhA, Bouwens JFH, Schuit GCA (1972) J Catal 25:1
5. Grasselli RK (2002) Top Catal 21:79
6. Linn WJ, Sleight AW (1976) J Catal 41:134
7. van Oeffelen DAG, van Hooff JHC, Schuit GCA (1985) J Catal 95:84
8. Oh SC, Lee HP, Kim HT, Yoo KO (1999) Korean J Chem Eng 16:543

9. Toledo-Antonio JA, Nava N, Matínez M, Bokhimi X (2001) Appl Catal A 234:137
10. Madeira LM, Portela MF (2002) Catal Rev 44:247
11. Kung HH (1994) Adv Catal 40:1
12. Chaar MA, Patel K, Kung HH (1988) J Catal 109:463
13. López Nieto JM, Concepción P, Dejoz A, Knözinger H, Melo F, Vázquez MI (2000) J Catal 189:147
14. Krishnan VV, Suib SL (1999) J Catal 184:305
15. Egashira M, Matsuo K, Kagawa S, Seiyama T (1979) J Catal 58:409
16. Batist PhA, Lippens BC, Schuit GCA (1966) J Catal5:55
17. Moro-oka Y, Ueda W (1994) Adv Catal 40:233
18. Jung JC, Kim H, Choi AS, Chung Y-M, Kim TJ, Lee SJ, Oh S-H, Song IK (2006) J Mol Catal A 259:166
19. Grzybowska B, Haber J, Komorek J (1972) J Catal 25:25
20. Hoefs EV, Monnier JR, Keulks GW (1979) J Catal 57:331
21. Wolfs MWJ, Batist PhA (1974) J Catal 32:25
22. He D-H, Ueda W, Moro-oka Y (1992) Catal Lett 12:35
23. Grasselli RK, Burrington JD (1981) Adv Catal 30:133
24. Kung HH, Kung MC (1985) Adv Catal 33:159
25. Ueda W, Asakawa K, Chen C-L, Moro-oka Y, Ikawa T (1986) J Catal 101:360
26. Jung JC, Kim H, Kim YS, Chung Y-M, Kim TJ, Lee SJ, Oh S-H, Song IK (2007) Appl Catal A 317:244
27. Jung JC, Lee H, Kim H, Chung Y-M, Kim TJ, Lee SJ, Oh S-H, Kim YS, Song IK (2008) Catal Commun 9:447
28. Ruckenstein E, Krishnan R, Rai KN (1976) J Catal 45:270
29. Schuit GCA (1974) J Less Comm Metals 36:329
30. Grasselli RK (1997) In: Ertl G, Knözinger H, Weitkamp J (eds) Handbook of heterogeneous catalysis, vol 5. Wiley, New York, Chapter 4
31. Batist PhA, Der Kinderen AHWM, Leeuwnburgh Y, Metz FAMG, Schuit GCA (1968) J Catal 12:45
32. Krenzke LD, Keulks GW (1980) J Catal 64:295
33. Dai HX, Ng CF, Au CT (2000) J Catal 189:52
34. Royer S, Duprez D, Kaliaguine S (2006) Catal Today 112:99
35. Jung JC, Lee H, Kim H, Chung Y-M, Kim TJ, Lee SJ, Oh S-H, Kim YS, Song IK (2008) Catal Commun 9:943